Respiratory Physiology & Neurobiology 185 (2013) 600–607

Contents lists available at SciVerse ScienceDirect

Respiratory Physiology & Neurobiology

journal homepage: www.elsevier.com/locate/resphysiol

Inhibition of rat carotid body glomus cells TASK-like channels by acute hypoxia is enhanced by chronic intermittent hypoxia

Fernando C. Ortiz[a], Rodrigo Del Rio[a], German Ebensperger[b], Victor R. Reyes[b], Julio Alcayaga[c], Rodrigo Varas[a], Rodrigo Iturriaga[a,*]

[a] Laboratorio de Neurobiología, Facultad de Ciencias Biológicas, P. Universidad Católica de Chile, Santiago, Chile
[b] Programa de Fisiopatología, ICBM, Facultad de Medicina, Universidad de Chile, Santiago, Chile
[c] Laboratorio de Fisiología Celular, Facultad de Ciencias, Universidad de Chile, Santiago, Chile

ARTICLE INFO

Article history:
Accepted 27 November 2012

Keywords:
Background K^+ channels
Glomus cells
Carotid body
Oxygen sensing
Obstructive sleep apnea

ABSTRACT

Chronic intermittent hypoxia (CIH), the main feature of obstructive sleep apnea, enhances carotid body (CB) chemosensory responses to acute hypoxia. In spite of that, the primary molecular target of CIH in the CB remains unknown. A key step of the hypoxic response in the CB is the chemoreceptor cell depolarization elicited by the inhibition of K^+ channels. Thus, we tested the hypothesis that CIH potentiates the hypoxic-induced depolarization of rat CB chemoreceptor cells by enhancing the inhibition of a background K^+ TASK-like channel. Membrane potential, single channel and macroscopic currents were recorded in the presence of TEA and 4-aminopyridine in CB chemoreceptor cells isolated from adult rats exposed to CIH. The CIH treatment did not modify the resting membrane properties but the hypoxic-evoked depolarization increased by 2-fold. In addition, the hypoxic inhibition of the TASK-like channel current was larger and faster in glomus cells from CIH-treated animals. This novel effect of CIH may contribute to explain the enhancing effect of CIH on CB oxygen chemoreception.

1. Introduction

Chronic intermittent hypoxia (CIH), which is the main feature of the obstructive sleep apnea (OSA) syndrome, is recognized as an independent risk factor for hypertension and other cardiovascular diseases (Somers et al., 2008). The current evidence shows that the CIH-induced potentiation of the carotid body (CB) chemosensory responses to acute hypoxia contributes to the OSA-induced hypertension (Iturriaga et al., 2009; Prabhakar and Kumar, 2010; Smith and Pacchia, 2007; Weiss et al., 2007). Indeed, patients with recently diagnosed OSA show enhanced sympathetic and cardiorespiratory responses to hypoxia, attributed to an increased CB chemoreflex response to hypoxia (Narkiewicz et al., 1998, 1999). Moreover, studies performed in animals models of OSA have shown that CIH enhances CB chemosensory and ventilatory responses to acute hypoxia (Del Rio et al., 2010; Pawar et al., 2009; Peng et al., 2003; Reeves et al., 2003; Rey et al., 2004), produces autonomic dysfunction (Prabhakar and Kumar, 2010; Rey et al., 2004, 2008; Zoccal et al., 2008) and induces a long-term potentiation of motor ventilatory activity (McGuire et al., 2004; Mitchell et al., 2001).

The mechanisms underlying the CIH enhancement of CB chemosensory reactivity to hypoxia are not entirely understood (Del Rio et al., 2011a,b; Iturriaga et al., 2009). Oxidative stress (Del Rio et al., 2010; Marcus et al., 2010; Peng et al., 2003), endothelin-1 (Pawar et al., 2009; Rey et al., 2006) and pro-inflammatory cytokines (Del Rio et al., 2011a; Iturriaga et al., 2009) have been associated with the carotid chemosensory potentiation. However, the primary molecular target responsible for the increased chemoreceptor discharge remains unknown (Iturriaga et al., 2009). The current model of CB chemoreception states that acute hypoxia depolarizes the chemoreceptor (glomus or type-I) cells, increasing intracellular [Ca^{2+}] and subsequently releasing one or more transmitters (Iturriaga and Alcayaga, 2004; Iturriaga et al., 2007). In neonatal rat glomus cells, the depolarization induced by hypoxia is initiated by the inhibition of a background K^+ current, which is likely due to the activity of the heterodimeric TASK-1/TASK-3 channel (Buckler, 1999, 2010; Kim et al., 2009). Accordingly, we hypothesized that CIH enhances CB chemosensory responses to acute hypoxia by increasing the inhibition of TASK-like channel activity, resulting in an increased membrane depolarization. Therefore, we studied whether CIH enhanced the inhibition of TASK-like channels and increased the amplitude of the hypoxic-induced depolarization in CB glomus cells isolated from rats exposed to CIH for 7 days, which show enhanced chemosensory and ventilatory responses to acute hypoxia (Del Rio et al., 2011a; Iturriaga et al., 2009). Finally, since functional TASK channels have not been

* Corresponding author at: Laboratorio de Neurobiología, Facultad de Ciencias Biológicas, P. Universidad Católica de Chile, Casilla 193, Santiago, Chile. Tel.: +56 2 686 2852; fax: +56 2 354 1850.
E-mail address: riturriaga@bio.puc.cl (R. Iturriaga).

1569-9048/$ – see front matter © 2012 Elsevier B.V. All rights reserved.
http://dx.doi.org/10.1016/j.resp.2012.11.015

reported in the Sprague Dawley rat adult CB glomus cells, we characterized the mRNA and protein expression as well as the electrophysiological distinctiveness of TASK channels in CBs of adult animals.

2. Materials and methods

2.1. Animals and ethical standards

Experiments were performed on adult male Sprague-Dawley rats (200–250 g, postnatal day ~90), fed with standard chow diet and kept on a 12-h light/dark schedule (8:00 am – 8:00 pm). Experimental procedures were approved by the Bioethical and Biosafety Committee of the Faculty of Biological Sciences of the Pontificia Universidad Católica de Chile and the Ethical Committee of the Facultad de Ciencias of the Universidad de Chile, and were conducted in accordance to the guidelines of the National Fund for Scientific and Technological Research (FONDECYT, Chile).

2.2. Experimental groups and exposure to chronic intermittent hypoxia

Rats were exposed to intermittent hypoxia as previously described (Iturriaga et al., 2009; Del Rio et al., 2010, 2011a,b). Unrestrained, freely moving rats were housed in individual chambers (12 cm × 35 cm, 3.96 L) and exposed to a CIH protocol consisting of hypoxic cycles of 5–6% inspired O_2 for 20 s, followed by room air for 280 s, applied 12 times/h, 8 h/day for 7 days. Rats have access to food and water ad libitum and the hypoxic pattern was applied during the daytime (8:00 am to 4:00 pm). The animals were kept in the chambers during 7 days, and were able to move freely and turn around in the chambers. Chambers were equipped with a rear inlet to admit N_2 and an extractor fan in the front. During normoxic periods the fans were continuously running, assuring low CO_2 levels in the chambers. During hypoxic exposure, the fans were stopped and solenoid valves allow 100% N_2 flow into the chambers. An automatized system controlled the solenoid valves and the alternating cycles of the fans. The O_2 level in the chambers was continuously monitored with an oxygen analyzer (Ohmeda 5120, USA). Rats of the control group were kept in the normoxic condition in the same room that rats were exposed to CIH. Room temperature was kept at 23–25 °C.

2.3. CB acute dissociation

CBs were surgically removed from the rats anesthetized with ketamine and xylazine (75/7.5 mg/kg) and placed in ice cold modified Hanks' balanced salt solution (pH 7.4 at 4 °C). The CBs were enzymatically (trypsin/collagenase) and mechanically dissociated as previously described (Buckler, 1997). The cellular suspension was plated onto poly-L-lysine (0.1 mg/mL) coated glass coverslips. Cells were kept at 37 °C in a culture chamber with air – 5% CO_2 in a water saturated atmosphere, until its use (2–8 h). The dissociated cells were used in electrophysiological and immunostaining studies.

2.4. Electrophysiological recordings

Electrophysiological studies were conducted using either cell-attached or whole-cell configuration in current-clamp or voltage-clamp mode with a patch clamp amplifier (Axopatch 200B, Molecular Devices, USA). Membrane current and voltage were filtered at 2 kHz and recorded at 20 kHz with a Digidata 1200 AD (Molecular Devices, USA). Microelectrodes were made from borosilicate glass capillaries and heat-polished before use (resistance 5–8 MΩ and seal resistance ≥ 5 GΩ). Cell-attached recordings were performed with several values of imposed pipette potential (Vp) to determine the I–V relationship. In the whole-cell voltage-clamp mode the macroscopic membrane current was recorded by imposing a voltage ramp from −120 mV to +20 mV (0.7 mV/ms, from a holding potential of −55 mV; see Fig. 1C inset). Current–clamp recordings were performed with no imposed current (I = 0, "voltage follower"). The coverslip with the platted cells was placed on a recording chamber (volume ~400 μL) on the stage of an inverted microscope, and continuously superfused with bath solution at 1.2–1.5 mL/min controlled with a two channel peristaltic pump (Masterflex CL, Cole Parmer, USA). For cell-attached and whole cell recordings, cells were superfused with a saline solution containing (in mM) 117 NaCl, 4.5 KCl, 23 $NaHCO_3$, 1 $MgCl_2$, 2.5 $CaCl_2$ and glucose 11, pH = 7.4 at 37 °C. The extracellular solution was equilibrated with 5% CO_2 in air (normoxia: PO_2 ~ 140 mmHg) or 5% CO_2 and 95% N_2 (hypoxia: PO_2 ~ 5 mmHg in the recording chamber). PO_2 of the solutions was monitored in the recording chamber with a 24 gauge oxygen needle electrode, connected to a polarographic chemical microsensor (Diamond Electro-Tech, USA). The cells were stimulated with the hypoxic solution for 30 or 90 s.

To isolate TASK currents, voltage-dependent K^+ currents present in glomus cells (Buckler, 1997; Buckler and Honoré, 2004) were blocked with 10 mM tetraethylammonium (TEA) and 5 mM 4-aminopyridine (4-AP) added either to the medium (whole cell) or to the internal pipette solution (cell-attached). No change on resting membrane potential (V_m) was observed when we applied TEA + 4-AP on bath solution (not shown). The pipette solution for cell-attached recordings contained KCl 140 or 70 mM (in ionic substitution experiments), 4 $MgCl_2$, 1 EGTA, 10 HEPES, 10 TEA and 5 4-AP, and equilibrated to pH = 7.4 at 37 °C. For whole cell recordings pipette solution was (in mM): KCl 140, $MgCl_2$ 1.5, MgATP 2, EGTA10, $CaCl_2$ 2, HEPES 10, pH 7.2.

Conventional intracellular recordings were performed to confirm the values of V_m recorded from CB glomus cells using the whole-cell configuration. Microelectrodes were made from borosilicate glass capillaries and backfilled with KCl 3 M (resistance: 30–60 MΩ). The microelectrodes were connected to an electrometer (IE-210, Warner Instruments, USA) and the signal was acquire at 20 kHz with the AxoScope 8.0 software. The entire CB was attached to the bottom of the recording chamber, and blind intracellular recordings were made from the whole CB. Impaled cells were classified as glomus cell when they respond with membrane depolarization to the hypoxic or acidic stimuli (puff of saline equilibrated at pH 6.5 with PIPES buffer). Only stable recordings lasting for more than 5 min were considered for the analysis.

2.5. RNA isolation and RT-PCR assays

Total RNA was extracted from two independent pools of CBs from 8 control and 8 CIH-treated rats, respectively, using Trizol (Invitrogen Life Technologies, CA, USA). cDNA was synthesized by reverse transcription using random hexamers and the Revert aid H Minus reverse transcriptase (Fermentas Life Sciences, Ontario, Canada). Procedures were carried out according to the manufacturer's instructions. Primers for amplification of partial DNA sequences from TASK-1, (Forward 5′-CACCGTCATCACCACAATCGA-3′ and Reverse 5′-TGCTCTGCATCACGCTTCTC-3′, accession number AF031384) and TASK-3 (Forward 5′-CAGTGGAAGTTCGCCGGGT-3′ and Reverse 5′-GCTTCCTCTGCAGGGCA-3′, accession number NM_053405) were derived from the corresponding rat genes. PCR amplification was carried out from cDNA synthesized from 0.1 μg of total RNA, with 1 U of Taq polymerase (Promega), 10 mM Tris–HCl pH 9.0, 50 mM KCl, 0.1% Triton X-100, 1.5 mM $MgCl_2$, 0.2 mM dNTP mix and 0.3 μM of each one of the primers. The PCR products and

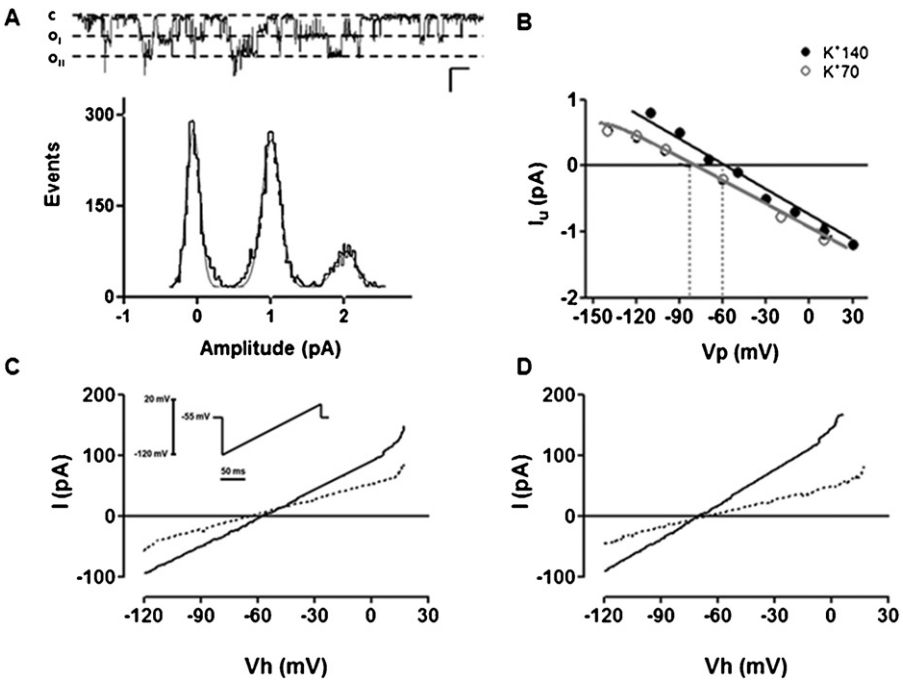

Fig. 1. Electrophysiological and pharmacological properties of TASK-like current in CB chemoreceptor cells from adult rats. (A) Cell-attached recording of channel current ($Vp = 0$ mV) in a CB glomus cell from an adult rat and its corresponding event-amplitude histogram (obtained from an all-point analysis). (C) Close level; OI, open level 1; OII, open level 2. Scale: 1 pA, 10 ms. (B) Effects of reducing pippete [K^+] from 140 mM (K^+140) to 70 mM (K^+70) on the unitary current (Iu) – pipette potential (Vp) relationship. The reduction of external [K^+] from 140 to 70 mM did not modify the single channel conductance (15.2 ± 0.6 pS K^+140 vs. 13.1 ± 0.2 pS in K^+70, $P > 0.05$, Mann Whitney test, $n = 4$ cells), displacing the inversion potential by 18.3 ± 0.2 mV, close to the expected value from the Nernst equilibrium (18.1 mV). (C) Extracellular acidification (pH 6.5; dotted line) reduced the macroscopic control (pH 7.4; solid line) conductance by ∼47% ($P < 0.05$, Mann–Whitney test, $n = 5$ cells), bath solution contained 10 mM TEA and 5 mM 4-AP (see Section 2) (D) Bupivacaine (200 μM; dotted line) reduced the macroscopic control (solid line) conductance by ∼60% ($P < 0.05$, Mann Whitney test, $n = 4$ cells), bath solution contained 10 mM TEA and 5 mM 4-AP (see Section 2).

molecular weight standard were separated by electrophoresis on ethydium bromide agarose gels and visualized under UV light.

2.6. Immunohistochemical and cytochemical detection of TASK-1 and TASK-3 potassium channel subunits

The TASK-1 and TASK-3 subunits in the rat CB were identified using immunohistochemistry. Briefly, anesthetized rats were perfused intracardially with phosphate buffer saline (PBS) at pH 7.4 for 10 min followed by buffered 4% paraformaldehyde (PFA, Sigma, USA). The carotid bifurcations containing the CB were dissected and post-fixed in PFA 4% for 12 h at 4 °C. Samples were then dehydrated in ethanol, included in paraffin, cut in 5 μm width sections, deparaffinized, rehydrated and mounted on silanized slides. Slides were submitted to microwave based antigen retrieval protocol (700 W for 6 min in citrate buffer 1 M, pH 6.0) for unmasking antigens which have become modified by the tissue fixation process. Samples were incubated with 0.3% H_2O_2 to inhibit endogenous peroxidase and then in a universal ready to use blocking solution (Vectastain Elite ABC Kit, Vector Lab, USA). The slides were incubated overnight at 4 °C in humidity chambers with specific antibodies for detection of TASK-1 (rabbit polyclonal antibody 1:100 anti-TASK-1, #APC-024, Allomone Labs, Israel) and TASK-3 (rabbit polyclonal 1:100 anti- TASK-3, #APC-044, Allomone Labs, Israel) subunits. Negative controls were performed by preadsorbtion of the primary antibody with the proper control peptide. After rinsing slides in cold PBS, samples were incubated with proper secondary antibodies conjugated with biotin followed by a ready-to-use stabilized ABC reagent (Vectastain Elite ABC Kit, Vector Lab, USA), and revealed at 37 °C in a dark chamber with 3,3-diaminobenzidine tetrahydrochloride (DAB; Sigma, USA). To avoid false positives during DAB chromogen quantification, special attention was kept to prevent DAB signal saturation. Finally, samples were counterstained with Harris Hematoxylin and permanently mounted with Entellan® (Merck, USA). Photomicrographs of the CB tissue were taken at 100× with a CCD-camera coupled to an Olympus CX 31 microscope (Olympus Corp., Japan), digitized and analyzed with the ImageJ software (NIH, USA). A color deconvolution algorithm was used to separate the Harris Hematoxylin and DAB staining, and quantify the immunoreactive (-ir) mark from the RGB (red–green–blue) images.

In another set of experiments, immunocytochemical detection of TASK subunits in CB glomus cells was performed. Isolated glomus cells were plated onto poly-L-lysine (0.1 mg/mL) coated 10 mm glass coverslips and fixed in 4% PFA for 10 min. Coverslips were then incubated for 12 h at 4 °C with a mixture of anti-TASK-1 antibodies (rabbit polyclonal antibody 1:100, number APC-024, Allomone Labs, Israel) or anti-TASK-3 antibodies (rabbit polyclonal 1:100, number APC-044, Allomone Labs, Israel) and anti-tyrosine hydroxylase (mouse monoclonal antibody 1:200 anti-TH, number MAB318, Millipore, USA), the latter used as a positive control for CB glomus cells recognition. After washing with cold (4 °C) PBS, cells were sequentially incubated with a mixture of fluorescent conjugated secondary antibodies anti-rabbit IgG (AlexaFluor488, Molecular Probes, USA) and anti-mouse IgG (AlexaFluor594, Molecular Probes, USA). Finally, the preparations were mounted in a fluorescent mounting media (Vectashield, Vector Labs, USA) and slides were observed in a Nikon Eclipse E epifluorescence microscope connected to a CCD camera.

2.7. Data and statistical analyses

Single channel recordings were analyzed with the pClamp 7.0 software (Molecular Devices, USA). Channel activity was reported

as the open probability times the number of channels in a given patch (NPo). Open events were defined using a threshold crossing method set at 50% of the main conductance level (defined from all-point histograms). Since the number of channels in a given patch may differ, the effect of hypoxia was standardized as the percentage of channel activity during normoxia. Analyses of inter-event and dwell time histograms for the first open level were performed for cell-attached recordings. The curves were fitted to a simple exponential equation to obtain the characteristic time constant (τ). Whole-cell *I–V* curves were fit to the Goldman–Hodgkin–Katz equation for simple electrodiffusion of K^+ (Koizumi et al., 2010), which predicts that in asymmetric K^+ conditions the *I–V* curve for the K^+ current must shows a small outward rectification at more positive potentials (Hille, 2001).

Data was expressed as mean ± SEM. The number of cells (n) reported here corresponds to the number of cells from different CB preparations tested for a given treatment. Each data group was tested for normal distribution using D'Agostino and Pearson test. Two group comparisons were performed using Student t test (paired/unpaired) or Mann–Whitney test, to parametric and non-parametric data, respectively. Kruskal–Wallis test followed by Dunn's multiple comparisons post hoc was used to compare two or more non-parametric groups. Curves with two variation factors were compared with two-way ANOVA followed by a Bonferroni *post hoc* test. All statistical tests were performed with GraphPad Prism 4.03 software for Windows (GraphPad Software, San Diego CA, USA) and the level of significance was set at $P < 0.05$.

3. Results

3.1. Characterization of the TASK-like current in glomus cells from adult rats

In cell-attached recordings under conditions that allows isolation of TASK-like currents ($Vp = 0$ mV; pipette solution containing 140 mM KCl, 4 mM Mg^{2+} 10 mM TEA and 5 mM 4-AP, and 4.5 mM KCl in the bath solution), we routinely observed single channel openings with mean current amplitude of ~1 pA and rapid flickering openings (~1 ms) and burst discharges (Figs. 1A and 3A), similar to what has been described for a TASK channel in glomus cells from the neonatal rat (Buckler, 1999; Kim et al., 2011, 2009; Williams and Buckler, 2004). All-point histograms constructed from these recordings suggest that events with larger current amplitude were due to simultaneous openings of two or more of the same channels (Fig. 1A). The *I–V* curve for single channel conductance in 140 mM K^+ and 4 mM Mg^{2+} in the pipette showed an unitary channel conductance of 15.4 ± 0.8 pS (Fig. 1B; $n = 16$ cells). Confirmation that the recorded current was carried primarily by K^+ ions was obtained with pipettes containing 70 mM K^+ (Fig. 1B), which resulted in a shift of the current reversal potential to a membrane potential value close to the calculated by the Nernst equilibrium equation. Indeed, changing the pipette [K^+] from 140 to 70 mM produced a displacement of the reversal potential of +18.3 ± 0.2 mV ($n = 4$ cells), value in close agreement with the theoretical expected value of +18.1 mV. In addition, we tested the effects of acidification and the local anesthetic bupivacaine, which are known inhibitors of TASK channels (Buckler et al., 2000). The whole-cell K^+ current was reduced by acidification of the external solution. Indeed, as is shown in Fig. 1C the macroscopic conductance was reduced from 1.59 ± 0.04 nS at pH 7.4 to 0.85 ± 0.03 nS at pH 6.5 ($P < 0.05$, Mann–Whitney, $n = 5$ cells). Similarly, administration of bupivacaine (200 μM) reduced the macroscopic conductance from 1.94 ± 0.06 to 0.78 ± 0.04 nS ($P < 0.05$, Mann–Whitney, $n = 4$ cells; Fig. 1D).

3.2. mRNA and immunoreactive presence of TASK-1 and TASK-3 in glomus cells from adult rat CB

Since our functional evidences show the presence of TASK-like currents in glomus cells isolated from adult rat CB, we first detected specific mRNA for principal candidates TASK channels, named TASK-1 and TASK-3, and then used immunodetection techniques to verify the expression of the corresponding proteins. As is shown in Fig. 2A, the RT-PCR assay allowed the amplification of partial sequences of TASK-1 (~450 bp) and TASK-3 (~540 bp) cDNA in the adult rat CB. Additionally, the CB tissue was immunoreactive for TASK-1 and TASK-3 proteins. The immunoreactivity for TASK-1 and TASK-3 subunits was mainly confined to clusters of cells, which have been defined as glomus cells in classical light microscope studies. Indeed, most of the positive immunoreactivity was found in round to ovoid cells with prominent nuclei organized in clusters around blood vessels (Fig. 2B). It is worth noting that TASK-1 immunostaining was also observed in the walls of blood vessels. In isolated CB cells, we determined that glomus cells expressed TASK-1 and TASK-3 subunits. As is shown in Fig. 2C, TASK-1 and TASK-3 positive immunoreactivity co-localized with the glomus cell marker tyrosine hydroxylase.

3.3. Effect of CIH on the TASK-like current inhibition induced by acute hypoxia

Under normoxic conditions, CIH-treated glomus cells show an *I–V* relationship for TASK-like currents that is not different to the control one ($P > 0.05$, Two way ANOVA) showing a single channel conductance of 14.3 ± 0.8 pS and a reversal potential of −58.9 ± 2.6 mV ($n = 12$). Moreover, when comparing the histogram of inter-event intervals for the first open state of the channel (O_1 in Fig. 1A) from control and CIH-treated glomus cells showed that under normoxic condition there are no differences with >90% of the open events grouped in the 0–5 ms interval. Similarly, the dwell-time of opening for the O_1 level during normoxia did not differ among both groups ($\tau = 1.1 \pm 0.5$ ms for control group ($n = 12$) versus $\tau = 0.9 \pm 0.1$ ms for CIH group ($n = 9$); $P > 0.05$; Mann–Whitney).

Isolated glomus cells were exposed to hypoxic superfusion (PO_2 ~5 mmHg) for 30 s while recording TASK-like currents. The hypoxic stimulus produced a marked reduction of the channel activity (NPo) in control and CIH-treated glomus cells (Fig. 3), without significant changes in the current amplitude (Fig. 4A). The hypoxic inhibition of NPo in both groups was voltage-independent (not shown) and had no effects on the unitary current amplitude (Fig. 4A). We found that the hypoxic stimuli in control cells evoked a reversible inhibition of the standardized NPo of 62.3 ± 2.4% compared to the previous normoxic condition ($P < 0.05$, Kruskal–Wallis followed by Dunn's *post hoc* test, $n = 16$; Fig. 3B). In the cells from CIH-treated rats, the inhibition was 96.4 ± 1.5% compared with the previous normoxic condition ($P < 0.05$, Kruskal–Wallis followed by Dunn's *post hoc* test, $n = 12$ cells; Fig. 3B). Thus, acute hypoxia inhibition of TASK-like currents was significantly larger ($P < 0.05$, Student t test) in cells from CIH-treated than from control animals. Moreover, the inhibitory effect of acute hypoxia on NPo was faster in CIH-treated cells related to the control group (τ_{50} of 9.0 ± 0.4 s in 16 control cells vs. 2.3 ± 0.4 s in 12 CIH-cells; $P < 0.05$, Student t test; Fig. 3B).

In control cells the histogram of inter-event intervals for the first open state of the channel showed that >90% of the open events grouped in the 0–5 ms interval. During acute hypoxia, the distribution of the inter-event intervals changed to longer duration intervals, reaching up to 40 ms (Fig. 4B). Similarly, the dwell-time of opening for the O_1 level during normoxia ($\tau = 1.1 \pm 0.5$ ms; $n = 12$) was significantly reduced ($P < 0.05$; Student t test) by the

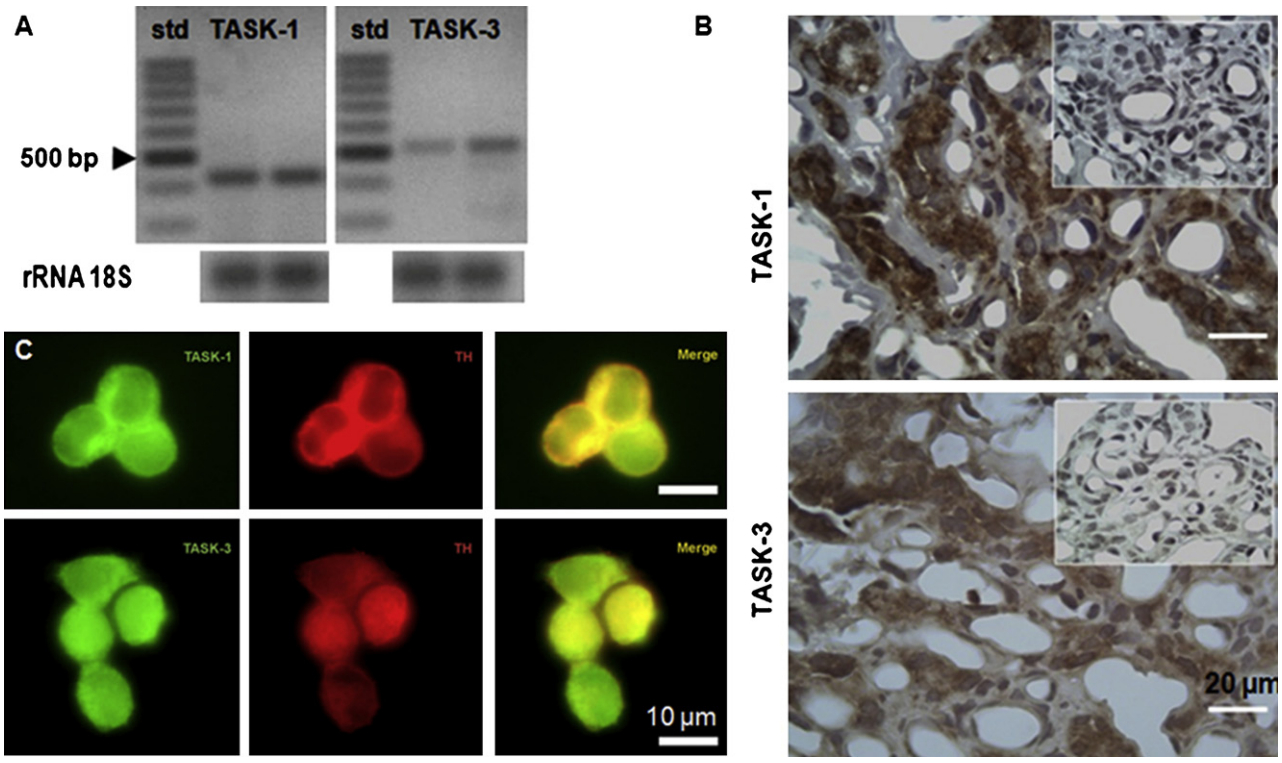

Fig. 2. Expression of TASK-1 and TASK-3 channel subunits in the CB chemoreceptor cells from adult rats. (A) cDNA bands corresponding to the amplification of TASK-1 and TASK-3 products of 450 base pairs (bp) and ~540 bp, respectively. Left row bp standards. Middle and right row duplicates of the CB samples. (B) Immunohistochemical staining for TASK-1 and TASK-3 subunits in the CB tissue from an adult rat. Inset, negative control. (C) Immunocytochemical detection of TASK-1 and TASK-3 subunits in isolated CB cells from an adult rat. Double-labeling of immunofluorescence for TASK-1 or TASK-3 (green) with the glomus cell marker tyrosine hydroxylase (TH, red), showing co-localization of the markers.

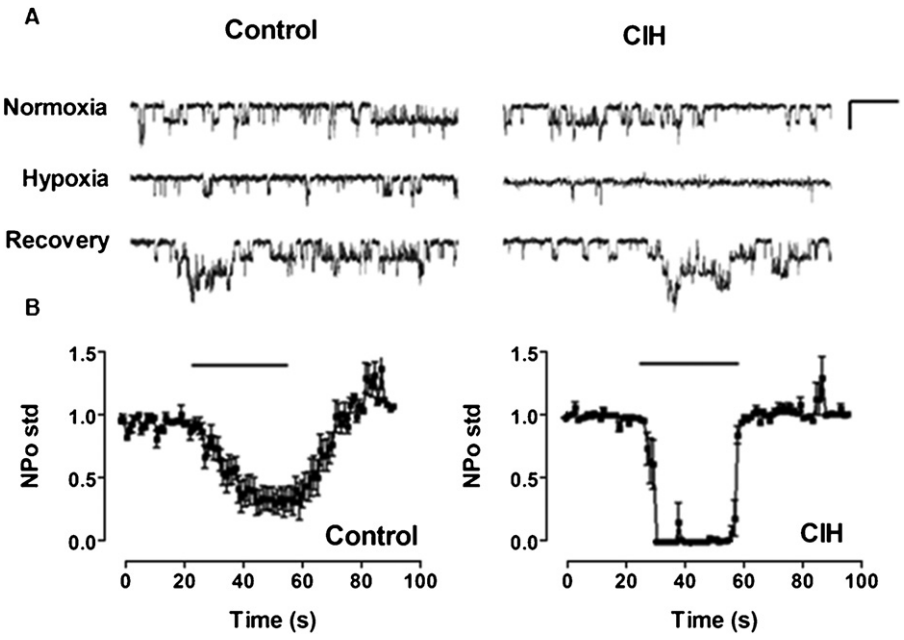

Fig. 3. Effect of CIH on the hypoxic-induced inhibition of TASK-like channels. (A) Cell-attached recording ($Vp = 0$ mV) of single channels from a control cell (left panel) and a CIH-treated cell (right panel) during normoxia, acute hypoxia ($PO_2 \sim 5$ mmHg) and recovery. Scale bar: 1 pA, 50 ms. (B) Time-course of the NPo inhibition induced by acute hypoxia (bar) in control cells (left panel) and CIH-treated cells (right panel). Acute hypoxia produced a larger and faster inhibition of the TASK-like channel open probability in cells from CIH rats. In 16 control cells the hypoxic stimulus evoked a reversible inhibition of the standardized NPo of 62.3 ± 2.4%, while in 12 cells from CIH group the inhibition was 96.4 ± 1.5% ($P < 0.01$, Mann–Whitney). The half-time to the maximum effect ($\tau 50$) was significantly ($P < 0.05$, Mann–Whitney test) faster in the CIH-treated cells (2.3 ± 0.4 ms; $n = 12$) than in control cells (9.0 ± 0.4 ms; $n = 16$). Note that only 30 s of stimulation was enough to trigger the NPo inhibition.

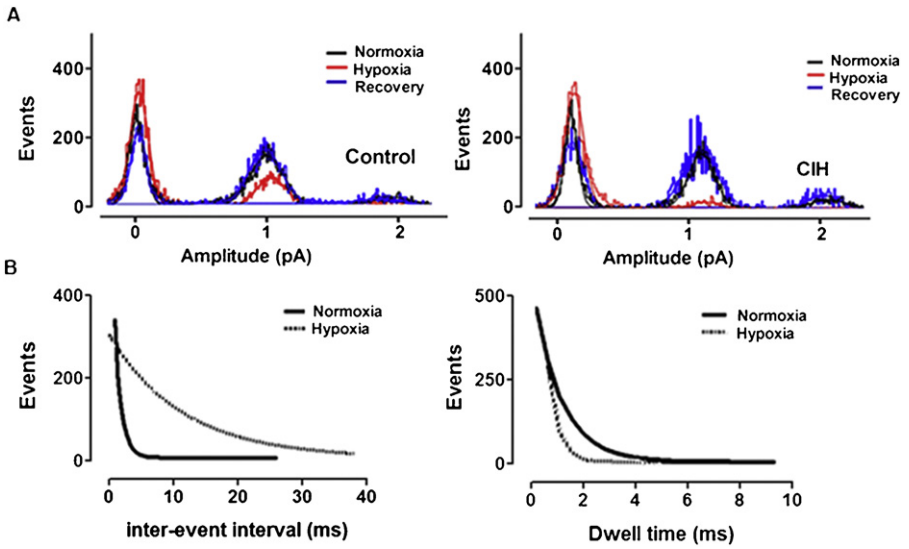

Fig. 4. Effect of CIH on TASK-like channel inhibition induced by acute hypoxia. (A) Amplitude histograms for channel recordings showed in Fig. 3A. In cells from control and CIH-treated rats the hypoxic stimuli decreased the number of open events without changing the current amplitude. (B) Inter-event interval and dwell-time histograms for the main open level in a control cell. Note that hypoxic stimuli modified the distributions of both the inter-event interval and dwell time.

Table 1
Resting membrane properties of adult CB glomus cells from control and CIH rats.

	Control	CIH
V_m (mV)	−54.5 ± 1.9 (58)	−50.1 ± 1.5 (22)
R_{in} (MΩ)	226 ± 68 (12)	291 ± 34 (20)
C_m (pF)	0.98 ± 0.3 (11)	1.1 ± 0.2 (18)

V_m, resting membrane potential, R_{in}, input resistance, C_m membrane capacity. No difference between control and CIH groups were observed ($P > 0.05$, Unpaired T test. Values correspond to average ± SEM. Number of recorded cells is indicated in brackets.

acute hypoxic challenge ($\tau = 0.4 \pm 0.1$ ms, $n = 12$). It should be noted that in spite of this value is near the limit of resolution given our loss-pass filter of 2 kHz we did not observed any effects on single events kinetics or burst hallmarks. Because TASK-like channel activity inhibition by acute hypoxia was larger than 95% in the CIH-treated cells, it was not possible to perform the equivalent analyses for these cells, since the minimum number of intervals or open sates (dwell time of opening) required to perform the analysis was not reached.

3.4. Enhanced TASK-like current inhibition induced by CIH contributed to increase the amplitude of the membrane depolarization evoked by acute hypoxia

We did not find any statistical difference in the resting membrane potential of glomus cells measured with conventional intracellular electrodes or with whole-cell configuration techniques (−54.3 ± 2.4 mV ($n = 30$) and −55.1 ± 1.4 mV ($n = 28$); respectively); therefore we pooled the data. CIH did not modify the resting membrane properties of CB glomus cells. No changes were observed neither in the resting membrane potential nor in the input resistance or in the glomus cell capacitance (Table 1).

Although the resting membrane potential was similar in both groups, the depolarization induced by acute hypoxia was enhanced by CIH exposure (Fig. 5A and C). Indeed, the amplitude of the depolarization evoked by hypoxia (ΔV_{Hx}) was 2-fold larger in cells from the CIH-animals compared to control cells ($\Delta V_{Hx} = 27.5 \pm 2.8$ mV in 16 CIH-cells vs. ΔV_{Hx} 15.7 ± 1.5 mV in 20 control cells; $P < 0.05$, Kruskal–Wallis, followed by Dunn's *post hoc*; Fig. 5A and C). Similarly, the amplitude of the depolarization evoked by acute hypoxia when K^+ voltage-dependent conductances were blocked by TEA and 4-AP in the bath solution was 3-fold higher in the CIH-treated cells as compared to the control group (32.9 ± 1.1 mV in 12 CIH-cells vs. 11.3 ± 0.8 mV in 17 control cells; $P < 0.05$, Kruskal–Wallis followed by Dunn's *post hoc*, Fig. 5B and C).

4. Discussion

4.1. General

We studied the effects evoked by CIH on the TASK-like channel activity and the depolarization induced by acute hypoxia in CB glomus cells from adult rats. The main findings of this study are that glomus cells of adult rats express TASK transcripts and proteins, as well as functional TASK-like currents, and the exposure to CIH for 7 days enhanced the hypoxic-induced inhibition of TASK-like channels in glomus cells. Indeed, the inhibition of the TASK-like channel opening probability (NPo) induced by acute hypoxia was more profound and faster in glomus cells of CIH-treated than in control rats. Similarly, although CIH did not modify the passive membrane properties of glomus cells in normoxia ($PO_2 \sim 140$ mmHg), the amplitude of the hypoxia-induced depolarization increased by 2-fold, and by 3-fold in the absence or presence of TEA and 4-AP. Thus, present results strongly support the idea that CIH increases the hypoxic-induced depolarization by enhancing the inhibition of TASK channels in glomus cell. Accordingly, this increased inhibition may contribute to the potentiation of the rat CB chemosensory responses to acute hypoxia found after 7 days of CIH exposure (Del Rio et al., 2011a; Iturriaga et al., 2009).

4.2. TASK channels in adult CB glomus cells

The participation of TASK channels in the CB hypoxic transduction process has been well established in the neonatal rat. Indeed, TASK-1, TASK-3 and TASK-1/3 heterodimers are functionally expressed in neonatal CB glomus cells, being the TASK-1/3 heterodimer the main hypoxic-sensitive conductance. Recently, Kim et al. (2011) reported that TASK channel activity in normoxic rat glomus cells did not differ between 0 and 16 days of birth, but hypoxic stimuli produced a progressive age-dependent decrease in TASK channel activity and a larger cell depolarization. The effect of

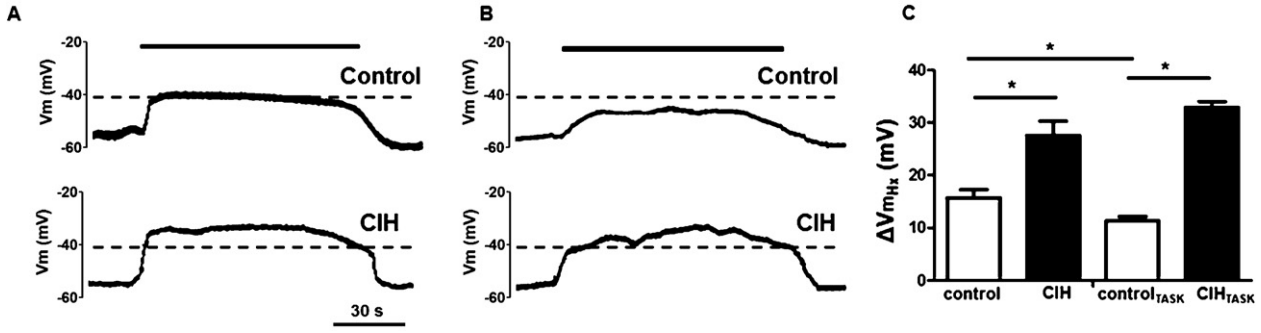

Fig. 5. Effect of CIH on CB cell depolarization induced by acute hypoxia. Recording of membrane potential during acute hypoxic stimuli (bar) in a control and in a CIH-treated cell in the absence (A) and presence (B) of 4-AP and TEA in the bath solution. (C) Summary of the effects of CIH on the CB cell depolarization evoked by acute hypoxia in standard solution (20 control and 16 CIH-treated cells) and in the presence of 4-AP and TEA (17 $control_{TASK}$ and 12 CIH_{TASK} cells). $^{*}P < 0.05$, Dunn test after Kruskal–Wallis test.

hypoxia on TASK channel activity was significantly larger in glomus cells from P16 to P18 when compared to cells obtained from P0 to P1 day old rats (Kim et al., 2011). In the present study, we demonstrated that TASK-like channels are functionally expressed in the rat glomus cells from ~90 days old rats, which present enhanced CB chemosensory and ventilatory responses to acute hypoxia after 7 days of CIH exposure (Del Rio et al., 2010; Iturriaga et al., 2009). Our conclusion that TASK-like channels are functionally expressed in CB cells from adult rats is based on several lines of evidence. The membrane current recorded in the presence of TEA and 4-AP was reversible inhibited by hypoxia in glomus cells from both control and CIH-treated rats, and therefore, could be involved in the adult CB hypoxic response to acute hypoxia. We found that the hypoxic challenges ($PO_2 \sim 5$ mmHg) evoked a reversible reduction of NPo of $62.3 \pm 2.4\%$ in glomus cells from adult control rats. This value is similar to the reported for the inhibition of TASK channels in glomus cells from neonatal rats (Buckler et al., 2000). In addition, the current recorded in CB cells from adult rats was inhibited by acidification and bupivacaine, and the reduction of pipette $[K^+]$ from 140 to 70 mM resulted in an expected displacement of the reversal potential according to the expected Nernst equilibrium potential for K^+ ions. The unitary channel conductance measured in our experiments, 15.4 ± 0.8 pS with 140 mM K^+ and 4 mM Mg^{2+} in the patch pipette, was also similar to the one reported for glomus cells from neonatal rats (Buckler et al., 2000; Williams and Buckler, 2004; Kim et al., 2009). Since we used 4 mM Mg^{2+} we cannot exclude the possibility that other TASK channels are present, such as the occasional 34 pS and 78 pS single channel conductances described by Kim et al. (2009) for the neonatal rat CB.

Similarly to what was found in Sprague-Dawley neonatal rats (Kim et al., 2006) and adult Wistar rats (Yamamoto et al., 2002), our immunohistochemical studies support that glomus cells from adult rats express the TASK-1 and TASK-3 channel subunits. Therefore, there is strong evidence showing that TASK-1 and TASK-3 are both expressed at the mRNA and protein levels in the rat CB.

4.3. Contribution of TASK-like channels to the CB chemosensory potentiation induced by CIH

Hypoxia causes depolarization of rat CB glomus cells, at least in part, by inhibiting the background TASK K^+ current (Buckler, 1997; Buckler et al., 2000). In order to establish a relationship between the increased hypoxic-inhibition of TASK-like channel open activity and the augmented depolarization observed in glomus cells from rats exposed to CIH, we studied the hypoxia-induced depolarization evoked by the inhibition of K^+ background conductance when the voltage-gated K^+ were blocked by TEA and 4-AP. In this condition, the depolarization evoked in the control cells was significantly smaller than the one observed in absence of the blockers. This observation is not surprising since several other voltage-dependent K^+ channels (i.e. BK or KO_2 channels) have been shown to be involved in the hypoxic response in glomus cells (López-Barneo et al., 1988; López-López et al., 1989; Peers, 1990). Thus, the depolarization evoked by hypoxia could be explained mainly by TASK channel inhibition (11.3 ± 0.8 mV of 15.7 ± 1.5 mV; Fig. 5) while the remaining response can be attributed to voltage-dependent K^+ channels blocked by TEA and/or 4-AP. Interestingly, when TEA and 4-AP were present in the bath solution, the depolarization induced by acute hypoxia was about 3-fold in glomus cells from CIH-treated animals, while only a 2-fold depolarization was observed in glomus cells from control rats. We ruled out the possibility that the CIH treatment increases TASK channel expression (and therefore enhanced depolarization) because an increased functional expression of a background K^+ conductance should necessarily reduce the input resistance and displace the resting membrane potential toward more negative values, scenario that we did not observed. Accordingly, CB type-I cells obtained from a mice deficient in TASK channels, show higher membrane resistance and less hyperpolarized resting membrane potential (Ortega-Sáenz et al., 2010). The finding that in the presence of TEA and 4-AP in the external solution, the depolarization induced by acute hypoxia was about 3-fold in glomus cells from CIH-treated animals strongly suggests that the enhanced depolarization observed in glomus cells from rats exposed to CIH was explained in part by a potentiation in the inhibition of TASK channel. The resting membrane properties of glomus cells were not modified by CIH, although a small but non-significant reduction of V_m was observed in cell from CIH-treated animals (-52.5 ± 1.5 mV; $n = 28$) with respect to control cells (-54.5 ± 1.9; $n = 58$). However, TASK-like channel conductance appears not to be modified by CIH, since the current amplitude distribution histogram in CIH and control glomus cells remain unchanged, suggesting that CIH has no direct effect on channel conductance. On the other hand, acute hypoxia in control glomus cells increased the inter-event interval to longer durations and reduced the dwell-time for the main open state of the channel, suggesting that acute hypoxia decreases channel activity by destabilizing the open state. Thus, CIH exposure may affect some regulatory factors involved in the hypoxic control of TASK-like channel activity, rather than having a direct effect on channel number or expression.

In summary, present results showed that (i) mRNA and protein of TASK channel subunits are present in rat adult glomus cells and (ii) CIH increased the acute hypoxia-induced inhibition of TASK-like K^+ channels, enhancing glomus cell depolarization. This novel effect of CIH may contribute to explain the enhancing effect of CIH on CB oxygen chemoreception.

Conflict of interest

No conflicts of interest, financial or otherwise are declared by the author(s).

Acknowledgements

This work was supported by grant 1100405 from the National Fund for Scientific and Technological Development of Chile (FONDECYT). Fernando Ortiz was supported by a CONICYT AT-fellowship.

References

Buckler, K.J., 1997. A novel oxygen-sensitive potassium–current in rat carotid body type I cells. Journal of Physiology 498, 649–662.

Buckler, K.J., 1999. Background leak K^+-currents and oxygen sensing in carotid body type 1 cells. Respiration Physiology 115, 179–187.

Buckler, K.J., 2010. Two-pore domain K^+ channels and their role in chemoreception. Advances in Experimental Medicine and Biology 66, 15–30.

Buckler, K.J., Honoré, E., 2004. Molecular strategies for studying oxygen-sensitive K^+ channels. Methods in Enzymology 381, 233–256.

Buckler, K.J., Williams, B., Honoré, E., 2000. An oxygen, acid- and anaesthetic sensitive TASK-like background potassium channel in rat arterial chemoreceptor cells. Journal of Physiology 525, 135–142.

Del Rio, R., Moya, E.A., Iturriaga, R., 2010. Carotid body and cardiorespiratory alterations in intermittent hypoxia: the oxidative link. European Respiratory Journal 36, 143–150.

Del Rio, R., Moya, E.A., Iturriaga, R., 2011a. Differential expression of pro-inflammatory cytokines, endothelin-1 and nitric oxide synthases in the rat carotid body exposed to intermittent hypoxia. Brain Research 1395, 74–85.

Del Rio, R., Moya, E.A., Muñoz, C., Arias, P., Court, F.A., Iturriaga, R., 2011b. Chronic intermittent hypoxia-induced vascular enlargement and VEGF upregulation in the rat carotid body is not prevented by antioxidant treatment. American Journal of Physiology Lung Cellular and Molecular Physiology 301, L702–L711.

Hille, B., 2001. Ion Channels of Excitable Membranes, 3rd ed. Sinauer Associates, Sutherland, MA, USA.

Iturriaga, R., Alcayaga, J., 2004. Neurotransmission in the carotid body: transmitters and modulators between glomus cells and petrosal ganglion nerve terminals. Brain Research Reviews 47, 46–53.

Iturriaga, R., Moya, E.A., Del Rio, R., 2009. Carotid body potentiation induced by intermittent hypoxia: implications for cardiorespiratory changes induced by sleep apnoea. Clinical and Experimental Pharmacology and Physiology 36, 1197–1204.

Iturriaga, R., Varas, R., Alcayaga, J., 2007. Electrical and pharmacological properties of petrosal ganglion neurons that innervate the carotid body. Respiratory Physiology and Neurobiology 157, 130–139.

Kim, D., Cavanaugh, E.J., Kim, I., Carroll, J.L., 2009. Heteromeric TASK-1/TASK-3 is the major oxygen-sensitive background K^+ channel in rat carotid body glomus cells. Journal of Physiology 587, 2963–2975.

Kim, I., Kim, J.H., Carroll, J.L., 2006. Postnatal changes in gene expression of subfamilies of TASK K^+ channels in rat carotid body. Advances in Experimental Medicine and Biology 580, 43–47.

Kim, D., Papreck, J.R., Kim, I., Donnelly, D.F., Carroll, J.L., 2011. Changes in oxygen sensitivity of TASK in carotid body glomus cells during early postnatal development. Respiratory Physiology and Neurobiology 177, 228–235.

Koizumi, H., Smerin, S.E., Yamanishi, T., Moorjani, B.R., Zhang, R., Smith, J.C., 2010. TASK channels contribute to the K^+-dominated leak current regulating respiratory rhythm generation in vitro. Journal of Neuroscience 30, 4273–4284.

López-Barneo, J., López-López, J.R., Ureña, J., González, C., 1988. Chemotransduction in the carotid body: K^+ current modulated by pO_2 in type I chemoreceptor cells. Science 241, 580–582.

López-López, J., González, C., Ureña, J., López-Barneo, J., 1989. Low pO_2 selectively inhibits K channel activity in chemoreceptor cells of the mammalian carotid body. Journal of General Physiology 93, 1001–1015.

Marcus, N.J., Li, Y.L., Bird, C.E., Schultz, H.D., Morgan, B.J., 2010. Chronic intermittent hypoxia augments chemoreflex control of sympathetic activity: role of the angiotensin II type 1 receptor. Respiration Physiology and Neurobiology 171, 36–45.

McGuire, M., Zhang, Y., White, D.P., Ling, L., 2004. Serotonin receptor subtypes required for ventilatory long-term facilitation and its enhancement after chronic intermittent hypoxia in awake rats. American Journal of Physiology Regulatory, Integrative and Comparative Physiology 286, R334–R341.

Mitchell, G.S., Powell, F.L., Hopkins, S.R., Milsom, W.K., 2001. Time domains of the hypoxic ventilatory response in awake ducks: episodic and continuous hypoxia. Respiration Physiology 124, 117–128.

Narkiewicz, K., Pesek, C.A., Kato, M., Phillips, B.G., Davison, D.E., Somers, V.K., 1998. Baroreflex control of sympathetic nerve activity and heart rate in obstructive sleep apnea. Hypertension 32, 1039–1043.

Narkiewicz, K., Van de Borne, P.J., Pesek, C.A., Dyken, M.E., Montano, N., Somers, V.K., 1999. Selective potentiation of peripheral chemoreflex sensitivity in obstructive sleep apnea. Circulation 99, 1183-1119.

Ortega-Sáenz, P., Levitsky, K.L., Marcos-Almaraz, M.T., Bonilla-Henao, V., Pascual, A., López-Barneo, J., 2010. Carotid body chemosensory responses in mice deficient of TASK channels. Journal of General Physiology 135, 379–392.

Pawar, A., Nanduri, J., Yuan, G., Khan, S.A., Wang, N., Kumar, G.K., Prabhakar, N.R., 2009. Reactive oxygen species-dependent endothelin signaling is required for augmented hypoxic sensory response of the neonatal carotid body by intermittent hypoxia. American Journal of Physiology Regulatory, Integrative and Comparative Physiology 296, R735–R742.

Peers, C., 1990. Hypoxic suppression of K^+ currents in type-I carotid-body cells-selective effect on the Ca^{2+}-activated K^+ current. Neuroscience Letters 119, 253–256.

Peng, Y.J., Overholt, J.L., Kline, D., Kumar, G.K., Prabhakar, N.R., 2003. Induction of sensory long-term facilitation in the carotid body by intermittent hypoxia: implications for recurrent apneas. Proceedings of the National Academy of Sciences of the United States of America 100, 10073–10078.

Prabhakar, N.R., Kumar, G.K., 2010. Mechanisms of sympathetic activation and blood pressure elevation by intermittent hypoxia. Respiratory Physiology and Neurobiology 174, 156–161.

Reeves, S.R., Gozal, E., Guo, S.Z., Sachleben Jr., L.R., Brittian, K.R., Lipton, A.J., Gozal, D., 2003. Effect of long-term intermittent and sustained hypoxia on hypoxic ventilatory and metabolic responses in the adult rat. Journal of Applied Physiology 95, 1767–1774.

Rey, S., Del Rio, R., Alcayaga, J., Iturriaga, R., 2004. Chronic intermittent hypoxia enhances cat chemosensory and ventilatory responses to hypoxia. Journal of Physiology 560, 577–586.

Rey, S., Del Rio, R., Iturriaga, R., 2006. Contribution of endothelin-1 to the enhanced carotid body chemosensory responses induced by chronic intermittent hypoxia. Brain Research 1086, 152–159.

Rey, S., Tarvainen, M.P., Karjalainen, P.A., Iturriaga, R., 2008. Dynamic time-varying analysis of heart rate and blood pressure variability in cats exposed to short-term chronic intermittent hypoxia. American Journal of Physiology Regulatory, Integrative and Comparative Physiology 295, R28–R37.

Smith, M.L., Pacchia, C.F., 2007. Sleep apnoea and hypertension: role of chemoreflexes in humans. Experimental Physiology 92, 45–50.

Somers, V.K., White, D.P., Amin, R., Abraham, W.T., Costa, F., Culebras, A., Daniels, S., Floras, J.S., Hunt, C.E., Olson, L.J., Pickering, T.G., Russell, R., Woo, M., Young, T., 2008. Sleep apnea and cardiovascular disease. Journal of the American College of Cardiology 52, 686–717.

Weiss, J.W., Liu, M.D., Huang, J., 2007. Physiological basis for a causal relationship of obstructive sleep apnoea to hypertension. Experimental Physiology 92, 21–26.

Williams, B.A., Buckler, K.J., 2004. Biophysical properties and metabolic regulation of a TASK-like potassium channel in rat carotid body type 1 cells. American Journal of Physiology Lung Cellular and Molecular Physiology 286, L221–L230.

Yamamoto, Y., Kummer, W., Atoji, Y., Suzuki, Y., 2002. TASK-1, TASK-2, TASK-3 and TRAAK immunoreactivities in the rat carotid body. Brain Research 950, 304–307.

Zoccal, D.B., Simms, A.E., Bonagamba, L.G., Braga, V.A., Pickering, A.E., Paton, J.F., Machado, B.H., 2008. Increased sympathetic outflow in juvenile rats submitted to chronic intermittent hypoxia correlates with enhanced expiratory activity. Journal of Physiology 586, 3253–3265.